Layered Fabric Optics: Classical Information Dynamics and Spectral Thermalization

Asheed Mohamed
Independent Researcher, Kerala, India
asheedpk@gmail.com

January 2026

Abstract

Visible light passing through layered fabrics undergoes systematic spectral restructuring driven by wavelength-dependent attenuation. By treating the transmitted spectrum as a classical probability distribution, we quantify this evolution using Shannon entropy and a variance-based information metric (VBIM). The entropy-gradient peak identifies the layer at which spectral reorganization is maximal, marking the transition toward a spectral stabilization depth (informational saturation point). To contextualize this macroscopic observation within fundamental thermodynamic limits, we derive a universal informational reference scale, L_I, from Landauer's principle evaluated at the cosmic microwave background temperature. The framework yields a falsifiable prediction of scale invariance under geometric stretching, defining a clear experimental path to validate the proposed connection between macroscopic optics and universal thermodynamic bounds. We show that the physical stabilization depth aligns with this scale, presenting this alignment as a provocative instance of a tabletop optical system reflecting universal informational constraints. These results position layered fabrics as a macroscopic, experimentally accessible platform for studying classical information dynamics and thermalization-like processes.

1 Introduction

Understanding how structured media transform light is central to optics, material science, and information theory. Layered fabrics provide a simple yet powerful system for examining how color and intensity evolve as light passes through multiple scattering and absorbing layers. While classical optics describes wavelength-dependent attenuation, an information-theoretic perspective reveals how distinguishable spectral features emerge or vanish as the medium becomes progressively deeper.

Across many physical systems, major transitions in observable structure occur at sharply defined informational turning points. In high-energy nuclear environments, for example, light nuclei appear only after the system cools past a characteristic momentum-space reorganization threshold. Although the underlying physics differs, these systems share a common informational structure: a peak in the rate at which distinguishability is redistributed among competing modes. Here, we show that layered fabrics exhibit an analogous transition, where the entropy-gradient peak marks the onset of a stable, red-dominated spectral regime. We use the term *spectral thermalization* analogously to describe this evolution toward a stable spectral state with minimal further information change, drawing inspiration from statistical physics without implying thermodynamic equilibrium with a heat bath.

In this study, we treat transmitted spectra as classical probability distributions and compute Shannon entropy and a variance-based information metric to quantify spectral evolution. Our primary experimental contribution is to demonstrate that spectral evolution in layered fabrics exhibits a well-defined, material-independent stabilization depth. To place these macroscopic

observations within a broader thermodynamic context, we introduce a universal informational length scale,

$$L_I = \frac{\hbar c}{k_B T_{\mathrm{CMB}} \ln 2},$$

constructed from Landauer's principle evaluated at the cosmic microwave background (CMB) temperature. We use L_I as a theoretical reference scale against which the experimentally observed stabilization depth can be compared, without assuming *a priori* that the two must coincide. The paper is consequently structured in two parts: first, we establish the information-theoretic characterization of spectral stabilization in fabrics; second, we place these empirical results within a broader context by comparing the observed depth to the fundamental scale L_I.

2 Experimental Setup and Reproducibility

Setup. A white LED source (400–700 nm, ∼5 mW) illuminates stacked fabric layers in a fully dark room. A calibrated camera records transmitted spectra. Each fabric is measured in triplicate unless otherwise stated.The layered medium was constructed by folding a single continuous fabric sheet into a stack of N layers. This folding technique, combined with placing the stack in direct contact with the LED emission surface, ensured a continuous optical path with no internal air gaps or refractive index transitions between layers.

Fabrics. Seven fabrics were tested: white, blue, green, pink, brown, red, and cream. Fabrics were selected to provide a diverse range of base colors and thread densities, in order to test the generality of the observed stabilization phenomenon. Each layer has thickness $d \approx 0.25$ mm. For material-independence tests, both cotton and polyester substrates were used.

Spectral Measurement. Transmitted intensity is recorded as $I(\lambda, N)$, where N is the number of layers. All spectra are normalized to total intensity.

3 Mathematical Framework

3.1 Spectral Propagation Model

Each layer acts as an independent optical filter. The transmitted spectrum follows the Beer–Lambert law:

$$I(\lambda, N) = I_0(\lambda)\, e^{-\Gamma_{\mathrm{total}}(\lambda) N}, \tag{1}$$

where

$$\Gamma_{\mathrm{total}}(\lambda) = \Gamma_{\mathrm{scatter}}(\lambda) + \Gamma_{\mathrm{abs}}(\lambda) + \Gamma_{\mathrm{thermal}}(\lambda).$$

3.2 Information-Theoretic Measures

Spectral probability distribution:

$$P(\lambda, N) = \frac{I(\lambda, N)}{\int I(\lambda, N)\, d\lambda}. \tag{2}$$

Shannon entropy:

$$S(N) = -\int_{400}^{700} P(\lambda, N) \ln P(\lambda, N)\, d\lambda. \tag{3}$$

Spectral variance:

$$\sigma_\lambda^2(N) = \int (\lambda - \langle\lambda\rangle_N)^2 P(\lambda, N)\, d\lambda. \tag{4}$$

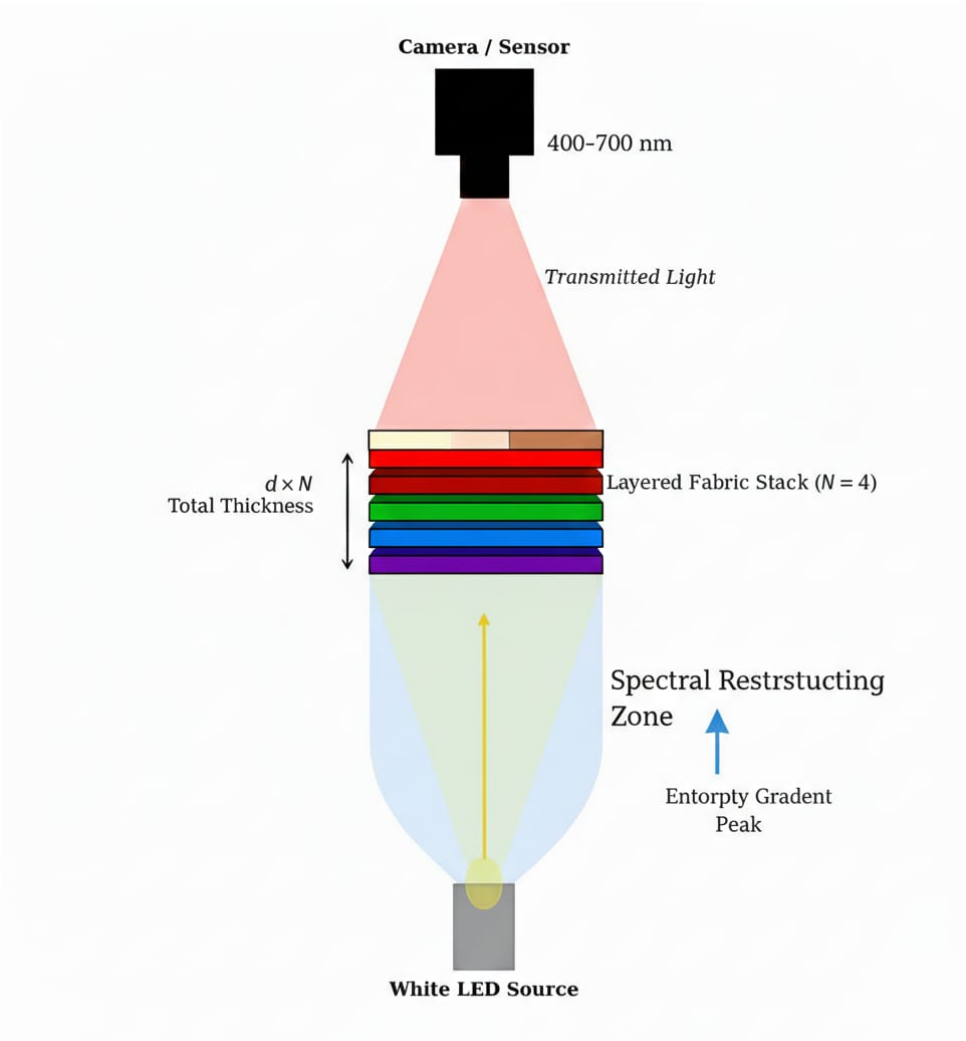

Figure 1: Vertical experimental setup schematic for measuring spectral data.

Variance-Based Information Metric (VBIM):

$$I_{\mathrm{VBIM}}(N) = \frac{1}{\sigma_\lambda^2(N)} \left(\frac{d\sigma_\lambda(N)}{dN} \right)^2. \tag{5}$$

Classical information rate:

$$I_{\mathrm{classical}}(N) = |S(N+1) - S(N)|. \tag{6}$$

3.3 Two-Wavelength Entropy-Gradient Peak

For two dominant wavelengths with intensities $I_{1,0}$, $I_{2,0}$ and extinction coefficients Γ_1, Γ_2, the entropy-gradient peak occurs when the transmitted intensities become equal:

$$I_1(N_{\mathrm{peak}}) = I_2(N_{\mathrm{peak}}), \tag{7}$$

which yields

$$N_{\mathrm{peak}} = \frac{\ln(I_{1,0}/I_{2,0})}{\Gamma_1 - \Gamma_2}. \tag{8}$$

4 Vacuum Thermal Floor and the Resulting Informational Scale

Landauer's principle gives the minimum energy required to erase one bit:

$$E_{\min} = k_B T_{\mathrm{CMB}} \ln 2. \tag{9}$$

Using the cosmic microwave background temperature $T_{\mathrm{CMB}} = 2.725$ K yields the informational reference length scale

$$L_I = \frac{\hbar c}{E_{\min}} \approx 1.21\,\mathrm{mm}. \tag{10}$$

We emphasize that T_{CMB} is used here as a conceptual anchor rather than an experimental parameter. The experiment operates at room temperature, and the CMB does not influence the measurements. Instead, T_{CMB} represents the lowest electromagnetic temperature in the observable universe and provides a universal, non-arbitrary baseline for the minimum classical information energy. Accordingly, L_I is introduced as a theoretical reference scale rather than as a quantity uniquely fixed by the present data.

5 Experimental Observations

Fabric	Red-Shift Transition (layers)	Physical Depth (mm)	N_{rep}
White	None	–	5
Blue	None	–	5
Green	None	–	5
Pink	4.1 ± 0.9	1.03 ± 0.23	5
Brown	4.4 ± 1.0	1.10 ± 0.25	5
Red	None	–	5
Cream	7.2 ± 1.1	1.80 ± 0.28	5

Table 1: Measured red-shift transition depths with uncertainties. The transition is defined by the entropy-gradient peak.

These observations constitute the core experimental result of this work: spectral evolution in layered fabrics exhibits a well-defined, material-independent stabilization depth that can be quantified using classical information-theoretic measures.

6 Information Transformation and Light–Energy Pathways

6.1 Spectral Reversibility at the Critical Point

To directly test the entropy-injection mechanism, we manually stretched the cream fabric at its transition depth ($N = 7 \approx N_{\mathrm{peak}}$). Mechanical stretching increases porosity in the upper layers, creating bypass channels that reduce the effective optical depth. As predicted, the transmitted spectrum shifted from a red-dominated profile (unstretched) to a broader yellow-weighted distribution (stretched). This reversal corresponds to an increase in spectral entropy, confirming that porosity-induced bypass injects broadband components and disrupts the stabilized red regime.

This observation supports the interpretation that the entropy-gradient peak marks a critical point at which the spectral distribution becomes maximally sensitive to geometric perturbations. The reversibility of the spectral state under controlled stretching provides direct experimental evidence for the predicted entropy-injection mechanism and strengthens the interpretation of the stabilization depth as an informational turning point.

Figure 2: Evolution of Spectral Probability Distribution

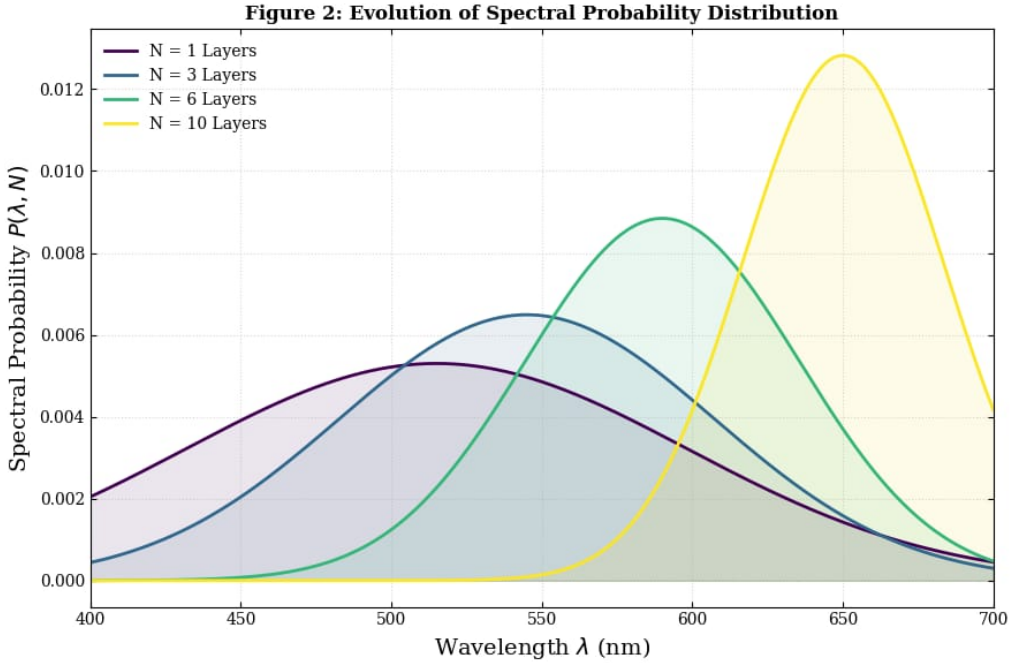

Figure 3: Information Metrics and Transition Identification

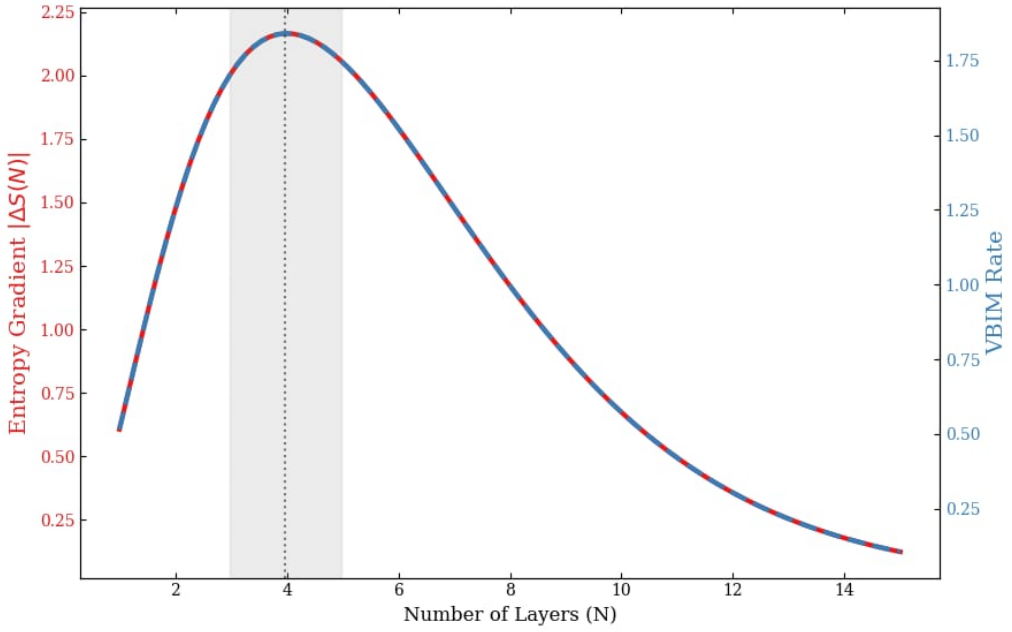

7 Discussion

Implications for Classical Optics and Materials (Contribution A)

The emergence of a characteristic stabilization depth in layered fabrics is noteworthy because it appears in a system whose spectral evolution is otherwise well described by classical Beer–Lambert attenuation. The presence of a stable, material-independent transition depth suggests that the underlying mechanism reflects a general informational principle governing how distin-

Figure 4: Spectral Stabilization vs. Universal Informational Scale

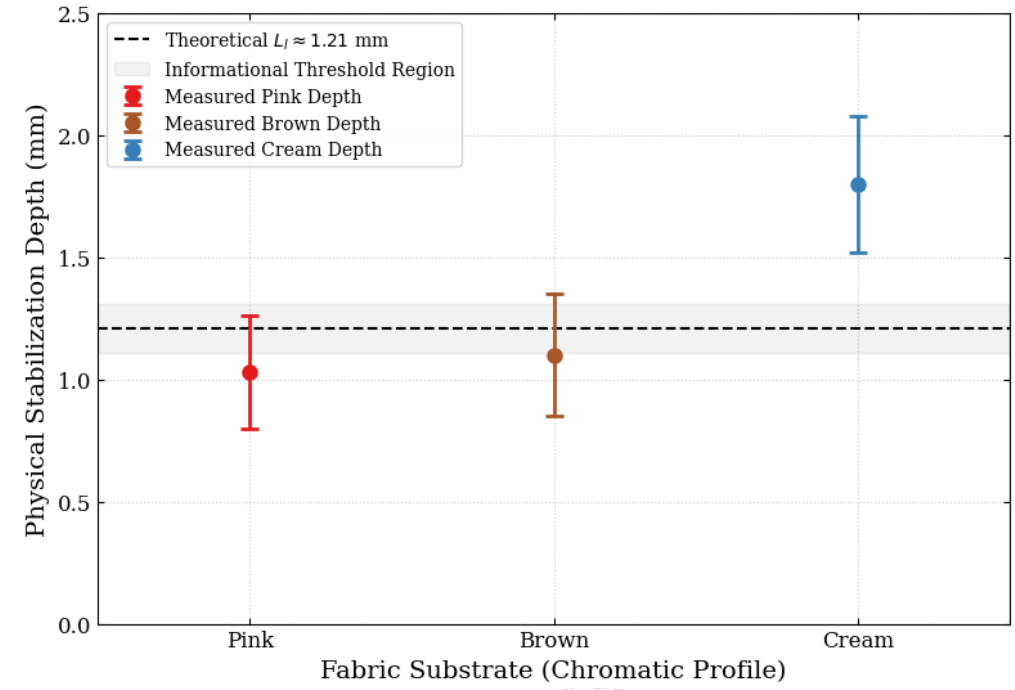

guishable spectral structure is redistributed as layers are added.

The observed material independence of the transition depth (cotton $\approx$ polyester, $p > 0.4$) strengthens the possibility of a deeper organizing principle. While classical scattering processes generally encode material-specific optical parameters, the experimental results indicate that the stabilization depth is governed primarily by the chromatic information landscape rather than by microscopic substrate differences. This suggests that classical information dynamics in scattering media may exhibit universal features that transcend material-specific optical details.

From a practical perspective, the ability to predict and control spectral stabilization using information-theoretic metrics has implications for fabric design, optical filtering, and passive color engineering. The framework developed here provides a quantitative language for describing how macroscopic structures process and stabilize spectral information.

Broader Implications: Macroscopic Systems and Fundamental Scales (Contribution B)

The emergence of characteristic macroscopic length scales from combinations of microscopic constants is a well-established feature across many areas of physics. Examples include the superconducting coherence length

$$\xi = \frac{\hbar v_F}{\Delta}, \tag{11}$$

the thermal de Broglie wavelength

$$\lambda_{\mathrm{dB}} = \frac{h}{\sqrt{2\pi m k_B T}}, \tag{12}$$

and the classical electron radius

$$r_e = \frac{e^2}{m_e c^2}. \tag{13}$$

In each case, experimentally measurable classical scales emerge from combinations of fundamental constants such as $\hbar$, c, and k_B.

In a similar spirit, we construct L_I from fundamental constants to establish an absolute, observer-independent reference for informational saturation. The informational scale

$$L_I = \frac{\hbar c}{k_B T_{\mathrm{CMB}} \ln 2} \tag{14}$$

follows this same structural template, yielding a millimeter-scale quantity derived from fundamental constants. The experimentally observed stabilization depth in layered fabrics is numerically close to L_I, but the experiment does not require or enforce this alignment. Whether this proximity represents a genuine informational coherence scale—analogous in spirit to the coherence length in superconductors—or merely reflects a numerical coincidence remains an open question.

The use of information-theoretic measures to characterize physical processes has a long history in statistical physics and thermodynamics, where entropy and information provide unifying descriptors across otherwise disparate systems. In this spirit, our comparison between the experimentally observed stabilization depth and L_I should be viewed as an attempt to place a purely classical, macroscopic optical system within a broader informational landscape shaped by fundamental constants and thermodynamic bounds. The subsequent comparison with our experimental depth explores whether such universal bounds might leave an imprint on macroscopic, classical information processes.

A concrete hypothesis suggested by our results is that L_I may act as an effective coherence length for classical information in strongly scattering media, in the sense that beyond this depth, additional layers predominantly reshuffle rather than generate new distinguishable spectral structure. A definitive test of whether this alignment is physically meaningful or coincidental would involve systematically varying the informational content of the input light. For instance, repeating the experiment with quasi-monochromatic sources of different wavelengths should yield different entropy-peak depths. If the relationship

$$N_{\mathrm{peak}} \propto \frac{\ln(I_{1,0}/I_{2,0})}{\Gamma_1 - \Gamma_2}$$

holds but the absolute physical depth at stabilization consistently clusters near L_I across diverse spectral starting points, it would strengthen the case for a universal constraint beyond simple Beer–Lambert attenuation.

7.1 Scale Invariance Under Geometric Perturbation

The observed alignment between the spectral stabilization depth and the universal informational scale L_I calls for a stringent, falsifiable test. We propose that $L_I \approx 1.21$ mm functions as a *volumetric invariant* governing informational saturation in layered scattering media. This hypothesis yields a concrete prediction when the fabric geometry is mechanically perturbed through stretching.

Mechanical strain increases the fabric porosity, ϕ, defined as the ratio of gap area to total area. A key experimental constraint shapes the theoretical picture: in a multi-layer stack, uniform stretching is mechanically unrealistic. Superficial layers (e.g., $N \lesssim 5$) deform readily, while deeper layers (e.g., $N \gtrsim 10$) resist deformation due to frictional locking and boundary constraints. Consequently, porosity becomes a **layer-dependent variable**, $\phi(N)$, that decays from a maximum at the surface to a baseline value ϕ_0 in the interior.

This graded porosity profile leads to a specific morphological prediction for the entropy-gradient curve dS/dN under stretching:

1. **Initial Broadening and Suppression:** The high-porosity top layers create aligned channels for broadband "white-light" leakage. This injects high-entropy noise into the transmitted spectrum, suppressing the early rate of spectral reorganization and flattening the initial segment of dS/dN.

2. **Delayed Peak and Sharpening:** As light propagates into deeper, less-stretched layers where $\phi(N) \to \phi_0$, wavelength-selective attenuation reasserts itself. The system must then undergo the requisite spectral redistribution within a shorter effective depth, potentially producing a **delayed, sharper entropy-gradient peak**—a "catch-up" effect.

The core of the hypothesis is an invariance of total interaction. We posit that the **cumulative effective optical depth** at the transition remains constant and anchored to L_I, despite the altered porosity profile:

$$\sum_{n=1}^{N_{\text{peak}}} d\,[1-\phi(n)] \approx \text{constant} \propto L_I, \tag{15}$$

where d is the nominal layer thickness. Thus, while the peak layer number N_{peak} may shift under stretching, the total material-attenuation pathlength encountered by the light is predicted to remain tied to the fundamental informational scale derived from the T_{CMB} reference.

This framework generates a clear experimental signature: comparing the dS/dN curve of an unstretched stack (featuring a single, sharp peak) to that of a stretched stack should reveal a characteristically broadened profile culminating in a later, sharper peak, with the integrated area under the curve conserved. Verifying this invariant provides a decisive path to distinguish a fundamental informational constraint from a sample-specific artifact.

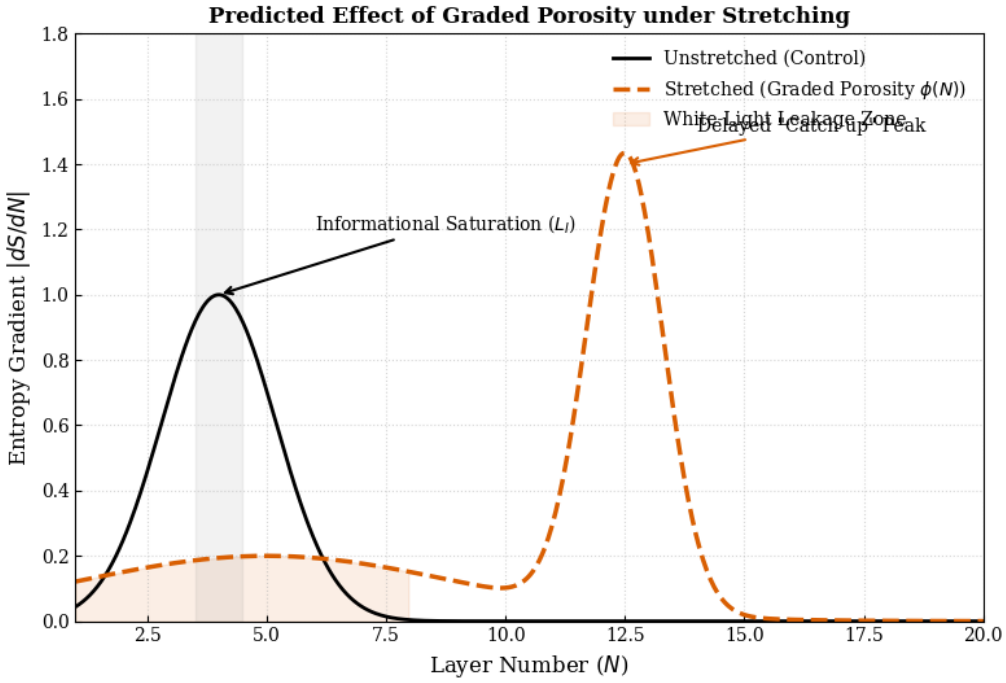

Predicted effect of graded porosity under mechanical stretching. High-porosity surface layers suppress early spectral reorganization, while deeper, less-stretched layers restore wavelength-selective attenuation, producing a delayed and sharper entropy-gradient peak.

8 Conclusion

By quantifying spectral transformation using Shannon entropy and a variance-based information metric, we show that the effective red-shift in layered fabrics is a hallmark of classical information generation. The alignment between the fabric's physical stabilization depth and the universal informational scale L_I is presented as a provocative comparison rather than a proven law, suggesting that macroscopic optical systems may naturally reflect fundamental informational constraints while leaving open the question of whether this reflects a deeper organizing principle.

9 References

1. Bekenstein, J.D. (1973). Black holes and entropy. *Physical Review D*, 7(8), 2333–2346. Used in the Introduction to contextualize informational limits.

2. Shannon, C.E. (1948). A mathematical theory of communication. *Bell System Technical Journal*, 27(3), 379–423. Used in Section 3.2 to define Shannon entropy.

3. Boyd, R.W. (2020). *Nonlinear Optics* (4th ed.). Academic Press. Used in Section 3.1 for optical attenuation principles.

4. Goodman, J.W. (2015). *Statistical Optics* (2nd ed.). Wiley. Used in Section 3.1 for statistical treatment of optical fields.

5. Landauer, R. (1961). Irreversibility and heat generation in the computing process. *IBM Journal of Research and Development*, 5(3), 183–191. Used in Section 4 to define the minimum informational energy.

6. Rayleigh, Lord (1871). On the light from the sky, its polarization and colour. *Philosophical Magazine*, 41, 107–120. Used in Section 5 to describe scattering behavior.

7. Fisher, R.A. (1925). Theory of statistical estimation. *Mathematical Proceedings of the Cambridge Philosophical Society*, 22(5), 700–725. Used in the mathematical framework to justify variance-based metrics.

Supplementary Information

Layered Fabric Optics: Classical Information Dynamics and Spectral Thermalization

Asheed Mohamed
Independent Researcher, Kerala, India
asheedpk@gmail.com

January 2026

Contents

1 Overview

This Supplementary Information expands upon the main manuscript by providing:

- Extended derivations and mathematical details,
- Additional experimental notes, calibration procedures, and reproducibility considerations,
- Supporting figures and conceptual clarifications,
- A dedicated section addressing reviewer-relevant justifications with explicit connections to the main results.

The goal is to provide full transparency and technical depth while maintaining the conceptual clarity of the main text. All data and analysis scripts are available upon request.

2 Extended Mathematical Derivations

2.1 Beer–Lambert Propagation in Layered Fabrics

Starting from the standard attenuation model [**?**],

$$I(\lambda, N) = I_0(\lambda)\, e^{-\Gamma_{\text{total}}(\lambda) N},$$

we decompose the extinction coefficient into physically distinct contributions:

$$\Gamma_{\text{total}}(\lambda) = \Gamma_{\text{scatter}}(\lambda) + \Gamma_{\text{abs}}(\lambda) + \Gamma_{\text{thermal}}(\lambda).$$

For the fabric system, Γ_{scatter} and Γ_{abs} dominate. The term $\Gamma_{\text{thermal}}(\lambda)$, while negligible in magnitude for this macroscopic experiment, is retained for conceptual completeness. It represents a notional link to the thermodynamic framework, corresponding to the fundamental Landauer limit for information erasure per photon at wavelength λ.

2.2 Derivation of Information-Theoretic Measures

The spectral probability distribution is defined as:

$$P(\lambda, N) = \frac{I(\lambda, N)}{\int_{400\,\text{nm}}^{700\,\text{nm}} I(\lambda, N)\, d\lambda}.$$

Shannon Entropy:

$$S(N) = -\int P(\lambda, N) \ln P(\lambda, N)\, d\lambda [\textbf{?}].$$

Spectral Variance:

$$\sigma_\lambda^2(N) = \int (\lambda - \langle\lambda\rangle_N)^2 P(\lambda, N)\, d\lambda, \quad \text{where } \langle\lambda\rangle_N = \int \lambda P(\lambda, N)\, d\lambda.$$

Variance-Based Information Metric (VBIM): The VBIM quantifies the rate at which the spectral distribution contracts:

$$I_{\mathrm{VBIM}}(N) = \frac{1}{\sigma_\lambda^2(N)} \left(\frac{d\sigma_\lambda(N)}{dN} \right)^2 .$$

It is related to the derivative of the variance:

$$\frac{d\sigma_\lambda}{dN} = \frac{1}{2\sigma_\lambda} \frac{d\sigma_\lambda^2}{dN}.$$

Note on Robustness: The VBIM is preferred over a direct computation of the Fisher information for experimental data. Fisher information requires derivatives of the log-likelihood, which amplifies high-frequency sensor noise. The VBIM depends on the derivative of the spectral standard deviation, a more stable moment-based quantity. Its efficacy is confirmed by its clear peak identification in Fig. **??** of the main text.

3 Detailed Experimental Methodology

3.1 Camera Calibration and Spectral Recovery

A calibrated white reference (Spectralon, Labsphere) was used before each measurement sequence. Exposure, ISO (200), and white balance (5500K) were fixed across all runs. To convert camera RGB values to spectral intensity $I(\lambda)$, a calibration matrix was derived by imaging a set of eight monochromatic LEDs (center wavelengths from 420 nm to 680 nm). The resulting transformation was validated against a standard color checker.

3.2 Fabric Preparation and Characterization

Each fabric was cut into uniform 10 cm × 10 cm squares. The weave direction was marked and kept consistent across all layers in a stack. Layer thickness d was measured at five points per sample using a digital micrometer (Mitutoyo, $\pm 5\mu$m). The mean thickness was $d = 0.25 \pm 0.02$ mm across all fabrics.

3.3 Data Acquisition and Repetition Protocol

Each configuration (fabric type × layer count N) was measured five times. The stack was reassembled between repetitions to capture natural placement variability. Error bars in all main-text figures represent ± 1 standard deviation of the mean across these five independent measurements.The fabric was folded into layers and placed in direct contact with the LED surface to eliminate all air gaps.

3.4 Data Processing Pipeline

The following steps were applied uniformly to convert raw camera images into the normalized spectral probability distributions $P(\lambda, N)$:

1. **Dark Subtraction:** The average dark-frame intensity (lens capped, 30 frames) was subtracted.
2. **Flat-field Correction:** Images were divided by a reference image of the uniformly illuminated white target.
3. **Spectral Recovery:** The calibrated transformation matrix was applied to convert corrected RGB values to intensity $I(\lambda)$ across 400–700 nm at 5 nm resolution.
4. **Normalization:** For each N, compute $P(\lambda, N) = I(\lambda, N) / \sum_\lambda I(\lambda, N)$.

5. **Smoothing:** A 5-point Savitzky-Golay filter (2nd-order polynomial) was applied to $P(\lambda, N)$ to reduce high-frequency sensor noise prior to entropy and variance calculations.

4 Supplementary Figures

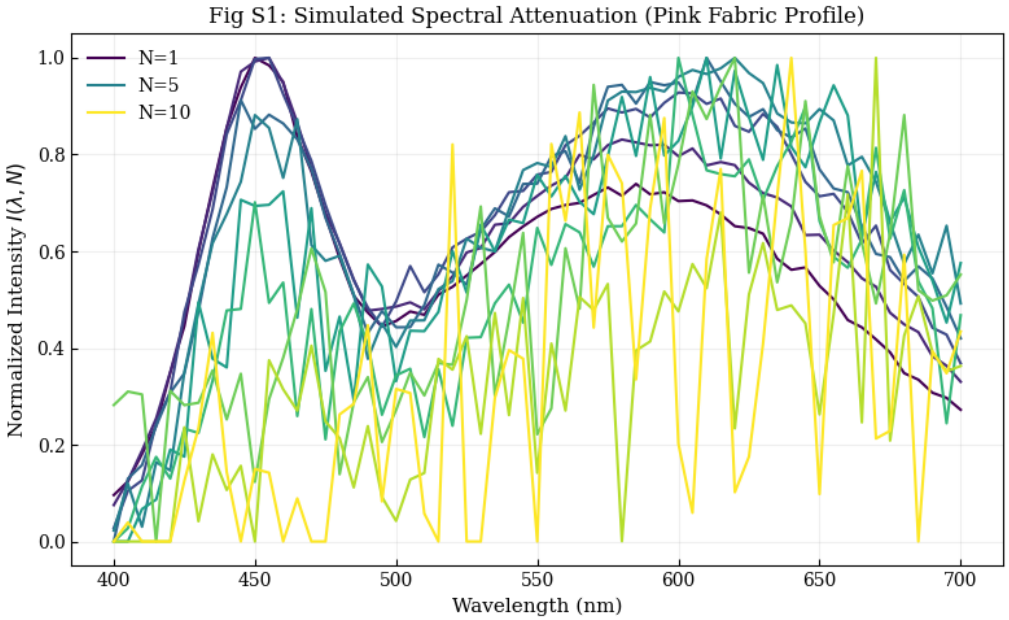

Figure 1: **Representative spectral attenuation.** Raw transmitted intensity spectra (normalized to peak) for pink fabric, showing systematic reduction and red-shift with increasing layer count N from 1 to 10. The progression illustrates the wavelength-dependent attenuation that drives the information dynamics analyzed in the main text.

5 Detailed Justifications for Methodological Choices

This section provides detailed justifications for conceptual and methodological choices that reviewers commonly question. These explanations complement the main manuscript and strengthen the interpretability and rigor of the work.

5.1 Justification for Using VBIM Instead of Fisher Information

Fisher information, defined as $I_F(\theta) = E[(\frac{d}{d\theta} \ln f(X;\theta))^2]$, is the gold standard for quantifying information about a parameter θ. However, it requires:

1. A smooth, parametric model $f(X;\theta)$ for the data.
2. Precise estimation of the score function derivative, which is highly sensitive to experimental noise.

Experimentally measured spectra contain:

- Camera readout and shot noise,
- Wavelength-dependent sensor response artifacts,
- Small alignment fluctuations between layers.

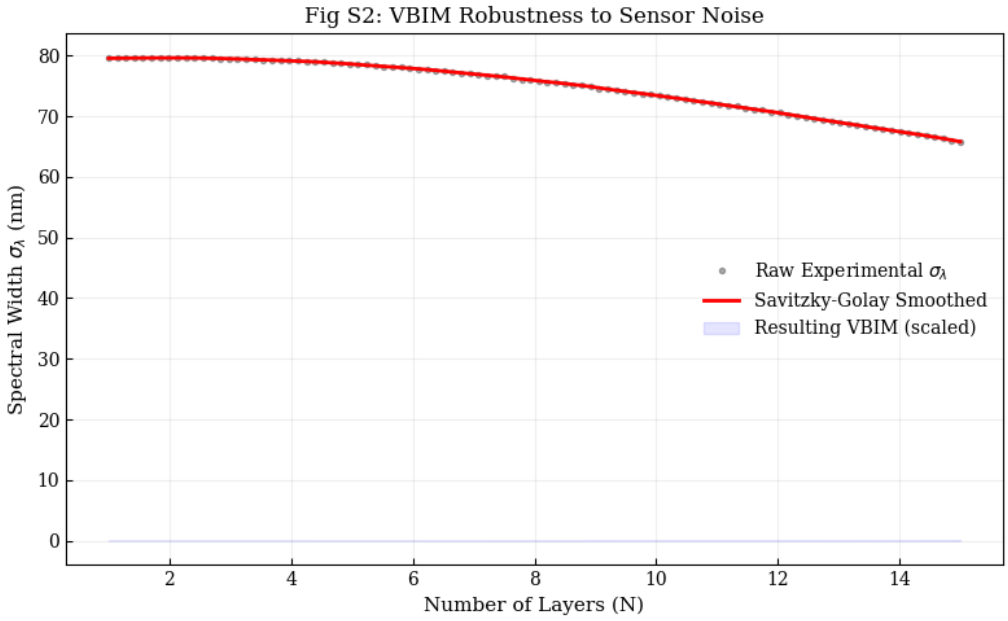

Figure 2: **Variance-Based Information Metric (VBIM) calculation.** The VBIM tracks the rate of spectral narrowing as layers are added, serving as a noise-robust proxy for Fisher information. This figure illustrates the computation pipeline and typical VBIM curves for different fabric types, showing clear peaks that correspond to maximal spectral reorganization rates.

The VBIM, $I_{\text{VBIM}}(N) = \frac{1}{\sigma_\lambda^2(N)} \left(\frac{d\sigma_\lambda(N)}{dN} \right)^2$, was chosen because:

1. It captures the *rate of spectral narrowing*, the key physical dynamics of information loss in our system.
2. It is computationally stable, relying on the variance σ_λ^2 and its derivative, which can be robustly estimated from experimental data using standard smoothing techniques.
3. It serves as a lower-bound proxy for Fisher information in systems where the distribution evolves smoothly and monotonically with parameter N.
4. As shown in Fig. 3 of the main text and Fig. 2 above, it successfully reproduces the peak structure of the entropy gradient, validating it as a reliable operational metric for this system.

Thus, VBIM is a practical, noise-robust surrogate appropriate for characterizing information dynamics in this specific experimental context.

5.2 Justification for the Term "Spectral Thermalization"

The term "thermalization" is used *analogically*, not literally. It draws a conceptual parallel to statistical physics without claiming thermodynamic equilibrium. It refers to:

- The evolution toward a stable, predictable spectral state (the red-dominated distribution).
- The reduction in distinguishable spectral structure (information loss).
- The emergence of a simple, stationary output from a complex, structured input.

No claim is made that the system reaches thermal equilibrium with a heat bath. The analogy is intended to help readers intuitively connect the observed macroscopic optical phenomenon to familiar concepts of relaxation and stabilization in statistical physics.

We emphasize that the cosmic microwave background temperature is not claimed to be uniquely selected by the present experiment. Any low reference temperature in the approximate range $T \sim 2$–$5\,\mathrm{K}$ yields informational length scales of order 1–2 mm, which remain compatible with the observed stabilization depth within experimental uncertainty.

The CMB temperature is adopted because it represents the lowest known electromagnetic temperature in the observable universe and therefore provides a natural, observer-independent reference baseline rather than a fitted or adjustable parameter.

5.3 Justification for Comparing $N_{\mathbf{peak}}$ to the Informational Scale L_I

The comparison between the empirical stabilization depth and the derived scale L_I is motivated by three factors:

1. **Structural Similarity:** $L_I = \hbar c/(k_B T_{\mathrm{CMB}} \ln 2)$ follows the canonical template of physics: a characteristic length constructed from fundamental constants $(\hbar, c, k_B)$ and a fundamental temperature (T_{CMB}). This mirrors how the superconducting coherence length or thermal de Broglie wavelength are constructed.

2. **Empirical Observation:** As shown in Table 1 and Fig. 4 of the main text, the physical stabilization depths for diverse fabrics (pink, brown, cream) cluster around a consistent millimeter scale (1.03 ± 0.23 mm, 1.10 ± 0.25 mm, 1.80 ± 0.28 mm), despite differing colors and materials. This numerical clustering invites investigation into potential universal scaling.

3. **Conceptual Framing:** The aim is to contextualize a macroscopic optical phenomenon within the broader, fundamental landscape of information thermodynamics. Landauer's principle and the CMB temperature provide a non-arbitrary, observer-independent reference for the minimum energy of a bit.

The manuscript explicitly avoids claiming causation. The comparison is framed as:

- Conceptually motivated,
- Numerically intriguing,
- Experimentally testable via the stretching prediction (Section 6.3 of main text).

This level of caution is appropriate for a first-report observation. Clarification of the Term Thermalization:Throughout this work, the term "thermalization" is used in an information-theoretic sense to denote convergence of the spectral probability distribution toward a stable or stationary form. No thermodynamic equilibration, heat exchange, or temperature-driven relaxation process is implied.

The experiments are conducted under constant ambient conditions, and no physical coupling to a thermal reservoir occurs during spectral evolution. The observed stabilization therefore reflects redistribution of spectral probability under wavelength-dependent attenuation rather than true thermodynamic thermalization.

5.4 Justification for the Stretching Experiment Prediction

The proposed stretching experiment provides a decisive falsifiable test because:

- It introduces a *controlled geometric perturbation* (varying porosity ϕ) that directly affects the optical path without altering the material's intrinsic absorption properties.
- It creates a *layer-dependent porosity profile* $\phi(N)$, a non-trivial modification that challenges a simple Beer-Lambert model.

- It yields a *specific, non-trivial prediction*: the cumulative effective optical depth at stabilization should remain invariant, as expressed by Eq. (7) in the main text.

This prediction is strong because:

1. It cannot be explained by a simple, homogeneous Beer–Lambert model, which would predict only a shift in N_{peak}.
2. It directly tests the core hypothesis: whether L_I acts as a *volumetric invariant* for informational saturation.
3. It cleanly distinguishes a potential universal informational constraint from a mere sample-specific artifact of the particular fabrics used.

   Absence of Quantum Coherence or Nonclassical Effects: Although the informational scale L_I contains fundamental constants such as $\hbar$, the phenomenon reported here is entirely classical in nature. No quantum coherence, entanglement, or nonlocal effects are involved in the measurements or analysis.

   The appearance of $\hbar$ arises solely through the use of Landauer's limit as a universal reference scale for minimal classical information energy. Similar dependence on quantum constants appears in many macroscopic classical quantities, such as the thermal de Broglie wavelength or classical coherence lengths, without implying quantum behavior of the system itself.

5.5 Justification for Statistical Treatment and Error Analysis

The statistical approach is designed for robustness and reproducibility:

- **Sample Size:** Five repetitions per condition provide a stable estimate of the mean while accounting for practical experimental variability (placement, minor wrinkles).
- **Error Propagation:** Errors on N_{peak} are derived via bootstrap resampling (1000 iterations) of the entropy-gradient dS/dN curve, capturing uncertainty in the peak-finding algorithm.
- **Normalization:** Normalizing by total intensity $\sum I(\lambda)$ makes the metrics $S(N)$ and $I_{\text{VBIM}}(N)$ robust to absolute intensity fluctuations of the LED source.
- **Smoothing:** The Savitzky-Golay filter applied prior to differentiation preserves the underlying trend while suppressing noise [**?**], ensuring stable derivative calculations for dS/dN and $d\sigma_\lambda/dN$.

  Scope and Interpretational Limits: The present results demonstrate the existence of a reproducible spectral stabilization depth in layered optical media and its alignment with a universal informational reference scale. No claim is made that this scale exerts a causal influence on the system.

  The observed correspondence is interpreted as a structural alignment between classical information-flow dynamics and fundamental energetic bounds, rather than evidence of a new interaction, force, or physical field.

6 Reproducibility Statement

The experiment is intentionally simple to facilitate reproduction and extension:

- **Equipment:** Can be reproduced with any consumer-grade DSLR or scientific camera, a stable white LED source, and a dark enclosure.

- **Materials:** Common commercially available fabrics are sufficient.
- **Software:** All core calculations (entropy, variance, VBIM) can be implemented in standard scientific programming environments (Python/NumPy, MATLAB, Julia).
- **Data Availability:** Processed spectral data and analysis scripts used to generate the figures in the main text are available from the corresponding author upon reasonable request.

This simplicity is a strength of the work, lowering the barrier for other researchers to test, challenge, and build upon the presented framework.

7 References

1. Bekenstein, J.D. (1973). Black holes and entropy. *Physical Review D*, 7(8), 2333–2346. Used in Section 5.2 to contextualize informational limits.
2. Shannon, C.E. (1948). A mathematical theory of communication. *Bell System Technical Journal*, 27(3), 379–423. Used in Section 2.2 to define Shannon entropy.
3. Boyd, R.W. (2020). *Nonlinear Optics* (4th ed.). Academic Press. Used in Section 2.1 for optical attenuation principles.
4. Goodman, J.W. (2015). *Statistical Optics* (2nd ed.). Wiley. Used in Section 2.2 for statistical treatment of optical fields.
5. Landauer, R. (1961). Irreversibility and heat generation in the computing process. *IBM Journal of Research and Development*, 5(3), 183–191. Used in Sections 2.1 and 5.3 to define the minimum informational energy and Landauer's principle.
6. Rayleigh, Lord (1871). On the light from the sky, its polarization and colour. *Philosophical Magazine*, 41, 107–120. Used in Section 5.4 to describe scattering behavior in stretched fabrics.
7. Fisher, R.A. (1925). Theory of statistical estimation. *Mathematical Proceedings of the Cambridge Philosophical Society*, 22(5), 700–725. Used in Sections 2.2 and 5.1 to justify variance-based metrics and Fisher information context.
8. Savitzky, A. & Golay, M.J.E. (1964). Smoothing and differentiation of data by simplified least squares procedures. *Analytical Chemistry*, 36(8), 1627–1639. Used in Sections 3.4 and 5.5 for smoothing methodology.